

Article

In Vitro and In Silico Screening Analysis of *Artabotrys sumatranus* Leaf and Twig Extracts for α -Glucosidase Inhibition Activity and Its Relationship with Antioxidant Activity

Dela Rosa ^{1,2} , Berna Elya ^{1,*} , Muhammad Hanafi ³, Alfi Khatib ⁴  and Muhammad Imam Surya ⁵ ¹ Department of Pharmacy, Faculty of Pharmacy, Indonesia University, Depok 16424, Indonesia² Department of Pharmacy, Faculty of Health Sciences, Pelita Harapan University, Tangerang 15811, Indonesia³ Chemistry Research Centre, National Research and Innovation Agency (BRIN), PUSPITEK, Serpong 15314, Indonesia⁴ Department of Pharmaceutical Chemistry, Kulliyah of Pharmacy, International Islamic University Malaysia, Kuantan 25200, Malaysia⁵ Research Center for Plant Conservation, Botanic Gardens, and Forestry, National Research and Innovation Agency (BRIN), Cianjur 43253, Indonesia* Correspondence: berna.elya@farmasi.ui.ac.id

Abstract: *Artabotrys sumatranus* is one of the *Artabotrys* species, which lives in Sumatera, Java, and Borneo in Indonesia. No research has been found related to its activity. The objective of this study was to explore the potential of *A. sumatranus* leaf and twig extracts as the source of an anti-diabetic agent through the α -glucosidase inhibition mechanism, as well as the relationship between the antioxidant and the α -glucosidase inhibition activities in these extracts. Ethanol extracts from leaf and twig *A. sumatranus* were subjected to several assays: total phenolic content, total flavonoid content, antioxidant activity using DPPH (2,2-diphenyl-1-picrylhydrazyl), radical scavenging activity, and FRAP (ferric reducing antioxidant power) analysis, as well as α -glucosidase inhibition. Later, GC-MS (gas chromatography-mass spectrometer) and LC-MS/MS (liquid chromatography-mass spectrometer/mass spectrometer) analysis were conducted to identify the compounds inside the extracts. The identified compounds were tested for potential α -glucosidase inhibition activity using a molecular docking simulation. As a result, the *A. sumatranus* leaf extract showed more potential than the twig extract as α -glucosidase inhibitor and antioxidant agent. In addition, from the comparison between the measured quantities, it can be deduced that most of the α -glucosidase active compounds in the *A. sumatranus* are also antioxidant agents. Several active compounds with a high affinity to α -glucosidase inhibition were identified using the molecular docking simulation. It was concluded that *A. sumatranus* twig and leaf extracts seem to be potential sources of α -glucosidase inhibitors.

Keywords: *Artabotrys sumatranus*; antidiabetic; antioxidant; leaf extract; twig extract

Citation: Rosa, D.; Elya, B.; Hanafi, M.; Khatib, A.; Surya, M.I. In Vitro and In Silico Screening Analysis of *Artabotrys sumatranus* Leaf and Twig Extracts for α -Glucosidase Inhibition Activity and Its Relationship with Antioxidant Activity. *Sci. Pharm.* **2023**, *91*, 2. <https://doi.org/10.3390/scipharm91010002>

Academic Editor: Valentina Onnis

Received: 6 November 2022

Revised: 11 December 2022

Accepted: 15 December 2022

Published: 22 December 2022



Copyright: © 2022 by the authors. Licensee MDPI, Basel, Switzerland. This article is an open access article distributed under the terms and conditions of the Creative Commons Attribution (CC BY) license (<https://creativecommons.org/licenses/by/4.0/>).

1. Introduction

Diabetes is a global health disorder which is marked by hyperglycemia and glucose intolerance, caused by a defective insulin function, defective insulin secretion, or both [1]. In the long term, diabetes can cause cardiovascular disease, kidney malfunction, and neuropathy [2]. One of the effective ways to cure diabetes type 2 is to inhibit α -glucosidase, an enzyme that catalyzes starch hydrolysis to simple sugars, so that the level of glucose in the blood can be maintained [3].

Not only to cure diabetes, inhibitors of α -glucosidase also have an effect on polysaccharide metabolism, glycoprotein processing, and cellular interaction, thus broadening the potential of α -glucosidase inhibitors as a treatment candidate for anti-viral diseases [4] and cancer [5]. Several α -glucosidase inhibitor synthetic drugs, such as acarbose, miglitol, and voglibose, have side effects in the gastrointestinal (GI) tract such as abdominal discomfort,

flatulence, and diarrhea. These side effects are caused by the carbohydrates which are not absorbed, and thus remain in the gut. Later on, the bacteria will digest the carbohydrates in the colon, which then produces gas [6,7]. Nevertheless, an α -glucosidase inhibitor can be used in a patient who is not tolerating other anti-diabetic agents because it is absorbed poorly, and its action is topical in the gut [8]. An α -glucosidase inhibitor is the first-line drug to treat a newly diagnosed type 2 diabetes patient [9].

Antioxidant activity can also help in the treatment of diabetes by inhibiting the deterioration of pancreatic β -cells caused by oxidative stress [10,11]. Defective insulin secretion from pancreatic β -cells can induce the most prevalent type of diabetes: diabetes mellitus type 2 [12]. It is therefore interesting to see whether there is a correlation between antioxidant activity and the α -glucosidase inhibitor.

Many research studies have explored antioxidant and α -glucosidase inhibitors from natural compounds [3,13,14]. The antioxidant compounds are mainly the phenolic and flavonoids groups [15], while α -glucosidase comes from different classes of secondary metabolites. For example, mangiferin and rutin belong to the flavonoid group [16,17], whereas 3-oxolupenal, which is isolated from *Nuxia oppositifolia*, is a lupane-type triterpenes [18]. Vasicine and vasicinol are examples of alkaloid compounds, which can inhibit alpha glucosidase [19], while procyanidin A2 is one of the α -glucosidase inhibitors from the tannin group [20]. Kotalanol, one of the strongest α -glucosidase inhibitors from plants, with an IC_{50} 0,58 μ g/mL [21,22], is a thiosugar sulfonium. The largest secondary metabolite class which contains α -glucosidase inhibitor compounds is the terpenes (the class of around 33% natural α -glucosidase inhibitors) [3].

Artabotrys is one of the biggest genera belonging to Annonaceae. It has more than 100 species in tropical Asia and Africa [23,24]. The plants of the Artabotrys genus are climbers, with characteristic inflorescence hooks [24]. Some Artabotrys plants are used as ethnomedicinals in several places; for example, the roots and stems of *Artabotrys suaveolens* are used as emmenagogues in the Philippines [25]. Despite the large number of varieties and the many ethnobotanical pharmaceutical uses, there has been only one study to explore the possibilities of using this genus as an anti-diabetic agent. This was done by Mohan et al. [26] on the methanol leaf extract of *A. suaveolens*. Most of the research on this genus was conducted to find its potential as anticancer [5,27–29] and anti-bacterial agents [25,30,31].

A. sumatranus is one of the Artabotrys species which lives in Sumatera, Java, and Borneo in Indonesia [24]. Until now, there has been no information regarding the phytochemical and biological activities in *A. sumatranus*. Therefore, the goal of this research was to explore the potential of this plant, especially the leaf and twig, as an α -glucosidase inhibitor, and its relationship with antioxidant activity.

2. Materials and Methods

2.1. Materials

Leaves and twigs of *A. sumatranus* (collection number C2009090117) were harvested from the collection of the Cibodas Botanical Garden in Cianjur (West Java, Indonesia). The collection was originally taken from the National Park Mount Leuser (latitude 03°50'02.9" N and longitude 97°31'17.2" E) in Aceh, Indonesia and was collected by Iyung and Wiguna Rahman.

The reagents used were ethanol (Smart Lab, Tangerang, Indonesia), Folin–Ciocâlteu (Merck, Darmstadt, Germany), sodium carbonate (Merck, Darmstadt, Germany), aluminum chloride (Smart Lab, Tangerang, Indonesia), gallic acid (Merck, Darmstadt, Germany), quercetin (Merck, Darmstadt, Germany), sodium acetate (Loba Chemie, Mumbai, India), 1,1-diphenyl-2-picrylhydrazyl (Smart Lab, Tangerang, Indonesia), ferric chloride hexahydrate ($FeCl_3 \cdot 6H_2O$) (Merck, Darmstadt, Germany), 2,4,6-Tris(2-pyridyl)-s-triazine or TPTZ (Sigma, St. Louis, MI, USA), hydrochloric acid (HCl) (Smart Lab, Tangerang, Indonesia), ferrous sulphate heptahydrate ($FeSO_4 \cdot 7H_2O$) (Merck, Darmstadt, Germany), acetic acid (Merck, Darmstadt, Germany), ascorbic acid (Merck, Darmstadt, Germany), α -glucosidase from *Saccharomyces cerevisiae* (Sigma, EC 232-604-7, St. Louis, MI, USA), p-nitrophenyl α -d-

glucopyranoside (Sigma, St. Louis, MI, USA), disodium hydrogen phosphate (Na_2HPO_4) (Merck, Darmstadt, Germany), sodium dihydrogen phosphate monohydrate (NaH_2PO_4) (Merck, Darmstadt, Germany), dimethyl sulfoxide (DMSO) (Merck, Darmstadt, Germany), sodium carbonate (Na_2CO_3) (Merck, Darmstadt, Germany), and distilled water.

The equipment used was: a freeze dryer (Alpha 1-2 LDplus Martin Christ, Osterode am Harz, Germany), rotary evaporator (Heidolph Hei-Vap Core, Schwabach, Germany), vortex (Reax Top Heidolph, Schwabach, Germany), incubator (Mettler IN55, Schwabach, Germany), UV spectrophotometer for α -Glucosidase Inhibition Assay (Thermo Fischer Scientific Varioskan Flash, Madison, WI, USA), UV spectrophotometer for other assays (Thermo Scientific Orion Aquamate 8000, Madison, WI, USA), gas chromatography—mass spectrometer (Agilent 7890B GC and 5777A MSD, St Clara, CA, USA) equipped with a capillary column ($30\text{ m} \times 250\ \mu\text{m} \times 0.25\ \mu\text{m}$, Agilent, type 19091S-433, St Clara, CA, USA), LC-MS-MS (Waters Acquity UPLC I-Class and XEVO G2-XS QToF, USA), and computer (Lenovo Legion 7, China) with the specifications AMD Reizen 7 5800H, RAM 32 GB, and graphic card NVIDIA GeForce RTX 3060, St. Clara, CA, USA.

The software used were Autodock version 4.2.6 and AutoDock tools version 1.5.7.

2.2. Extraction of *Artabotrys sumatranus*

The leaves and twigs were separated; each of them was dried by using a freeze dryer (Alpha 1-2 LDplus, Martin Christ), powdered, and macerated in ethanol solvent (1:5), for $2 \times 24\text{ h}$ at room temperature. The process was repeated twice. After maceration, the ethanol extract was then filtered, and the ethanol was evaporated using a rotary evaporator (Heidolph Hei-Vap Core) at $45\text{ }^\circ\text{C}$. The extracts obtained were then frozen and kept at $-20\text{ }^\circ\text{C}$ until further analysis.

2.3. α -Glucosidase Inhibition Assay

This assay was performed according to Dewi et al., (2014) [32]. The 0.1 M phosphate buffer was made by mixing 3.59 g Na_2HPO_4 , which was diluted in 100 mL distilled water, with 1.39 g NaH_2PO_4 , which was also diluted in 100 mL distilled water. NaH_2PO_4 was added until pH 7.0 was obtained. After that, distilled water was added until the total volume was 200 mL. Later, 250 μL of 5 mM P-nitrophenyl- α -D-glucopyranoside (PNPG) solution was mixed with 495 μL of 0.1M phosphate buffer (pH 7.0), and then was added to a reaction tube, which was filled with a 5 μL sample in DMSO with different concentrations. The solution was mixed homogenously and was incubated for 5 min at $37\text{ }^\circ\text{C}$. After that, 250 μL α -glucosidase (0.062 unit) was added and the solution was incubated for 15 min at $37\text{ }^\circ\text{C}$. To stop the reaction, 1mL of 0.2 M Na_2CO_3 was added. The absorbance was measured using a UV spectrophotometer (Thermo Fischer Scientific Varioskan Flash) at $\lambda = 400\text{ nm}$. PNPG and phosphate buffer were used as controls and quercetin as the positive control. The blank was DMSO. The absorbance reading of the blank was set to be zero. The percentage of α -glucosidase inhibition activity was calculated using:

$$\% \text{ Inhibition} = \frac{\text{Abs control} - \text{Abs sample}}{\text{Abs control}} \times 100\%$$

This assay was conducted with several concentrations in triplicate to get the IC_{50} value.

2.4. 2,2-Diphenyl-1-Picrylhydrazyl (DPPH) Radical Scavenging Activity Assay

This method was conducted based on González-Palma et al., (2016) [33], with some modifications. The samples were dissolved in ethanol and then mixed homogenously using the vortex. Then, 1 mL of DPPH 0.175 mM was added to 0.8 mL of the sample in the tube, and the mixture was vortexed until homogenous. The resulting sample mixture was incubated at room temperature in the dark for 30 min, and the absorbance was measured using the UV spectrophotometer (Thermo Scientific Orion Aquamate 8000) at $\lambda = 517\text{ nm}$. DPPH and ethanol were used as controls and ascorbic acid as the positive control. The

blank used was ethanol. The absorbance reading of the blank was set to be zero. The antioxidant activity was expressed in the percentage of DPPH reduction by the calculation:

$$\% \text{ reduction DPPH} = \frac{\text{Abs control} - \text{Abs sample}}{\text{Abs control}} \times 100\% \quad (1)$$

This assay was conducted for several concentrations in triplicate to get the IC₅₀ value.

2.5. Ferric Reducing Antioxidant Power (FRAP) Assay

The assay was performed based on Tomasina et al., (2012) [34] and Wiliantari et al., (2022) [35], with some modifications. For this assay, several types of Ferric Reducing Antioxidant Power (FRAP) solutions were needed: FRAP-1 to be used to make the standard calibration curve and FRAP-2 to be used with the extract samples and blank control.

The steps to make the FRAP-1 solution were as follows. First, the 10 mM TPTZ solution was prepared by dissolving 0.31 g TPTZ in 100 mL 40 mM HCl. Second, the acetate buffer, 300 mM (pH 3.6), was prepared by dissolving 0.16 g of sodium acetate in 100 mL of 0.28 M acetic acid. The pH level could be adjusted to reach 3.6 by adding 1 M HCl or NaOH. Third, 20 mM FeCl₃ solution was prepared by dissolving 0.135 g FeCl₃ in 25 mL distilled water. The FRAP-1 solution was made by mixing TPTZ (2,4,6-tri(2-pyridyl)-1,3,5-triazine) solution, distilled water, and acetate buffer (pH 3.6) with ratio 1:1:10.

To make the standard calibration curve, 1.68 mL of the FRAP-1 solution was added to 0.07 mL FeSO₄·7H₂O with different concentrations in distilled water. The mixture was vortexed until homogenous and incubated at 37 °C in the dark for 30 min. The absorbance of this mixture was then measured using the UV spectrophotometer (Thermo Scientific Orion Aquamate 8000) at λ = 593 nm. For the standard calibration curve, to nullify the effect of the FRAP-1 color, a blank (blank-1) was used, which was a mixture of 1.68 mL FRAP-1 and 0.07 mL distilled water (since the FeSO₄·7H₂O was dissolved in distilled water), and its absorbance was measured in the same way as for the FRAP-1 and FeSO₄ mixture. The difference between the absorbance of the mixture of FRAP-1 and FeSO₄·7H₂O, and the absorbance of blank-1 were plotted against the concentration of FeSO₄·7H₂O to make the standard calibration curve.

For the FRAP-2 solution, the TPTZ and buffer solutions were prepared as for the FRAP-1 solution. The difference is in the composition. The FRAP-2 solution was a mixture between TPTZ (2,4,6-tri(2-pyridyl)-1,3,5-triazine) solution, FeCl₃ solution, and acetate buffer (pH 3.6) with a ratio of 1:1:10.

To measure the samples (extract solution in ethanol with different concentrations), 1.68 mL of the FRAP-2 solution was added to a 0.07 mL sample, then the mixture was vortexed until homogenous and incubated at 37 °C in the dark for 30 min. The absorbance of this mixture was then measured using the UV spectrophotometer (Thermo Scientific Orion Aquamate 8000) at λ = 593 nm. The blank used for this sample measurement (blank-2), to nullify the effect of FRAP-2 color, was made by adding FRAP-2 solution to 0.07 mL ethanol (since the extract was dissolved in ethanol). The absorbance of blank-2 was measured in the same way as the mixture of FRAP-2 and sample. The difference between the absorbance of the mixture of the FRAP-2 and the sample and the absorbance of the blank-2 was recorded for different concentrations of extract.

The antioxidant activity was expressed as mM equivalents of Fe²⁺, or ferric ion equivalent antioxidant activity (FeEAc). The equivalency was obtained by using the standard calibration curve and comparing the concentration of FeSO₄·7H₂O with the concentration of extract for the same absorbance difference to the blanks. Ascorbic acid was used as the positive control, which was treated in the same way as the sample (replacing the sample with ascorbic acid). The result of the FRAP method can be reported in Fe²⁺ mol/g extract (similar to the units used in [36,37]), which can be computed using the following formula:

$$\frac{\text{Fe}^{2+} \text{ mol}}{\text{g}} = \frac{v_s}{1000} \times \frac{y_i - c}{x_i} \times \frac{1}{1000} \quad (2)$$

Here y_i is the concentration of Fe^{2+} equivalent in mM; x_i is the mass of the extracts in g (computed from the extract concentration in ppm); v_s is the tested sample volume in mL; and c is the intercept value of the regression line between the concentration of the Fe^{2+} equivalent in mM and the mass of the extracts in ppm.

For this assay, all the experiments were conducted in triplicate.

2.6. Total Phenolic Content

The total phenolic content was determined using the Folin–Ciocalteu method [38], with some modification. A 0.2 mL of sample was added to 1 mL of 10% Folin–Ciocalteu solution, vortexed until homogenous, and then incubated for 6 min at 25 °C. Later, the process was continued by adding 0.8 mL of saturated Na_2CO_3 to the test tube. The solution was mixed homogeneously using the vortex and incubated in the dark for 30 min at room temperature. The absorbance was measured at $\lambda = 765$ nm using the UV spectrophotometer (Thermo Scientific Orion Aquamate 8000). The total phenolic content was shown as milligrams of the gallic acid equivalent per gram of extract. The standard curve, which shows the relationship between the absorbance and concentration of the gallic acid, was made by replacing the sample with gallic acid. By using the regression line on the standard curve, and comparing the concentrations of gallic acid and extract for the same absorbance, the equivalent gallic acid concentration for a given extract concentration was obtained. The total phenolic content is shown as milligrams of the gallic acid equivalent per gram of extract (similar to the units used in [39,40]). This value was obtained by using the following formula:

$$\frac{\text{mg GAE}}{\text{g}} = \frac{1}{n} \sum_{i=1}^n \frac{y_i - c}{x_i} \times 1000 \quad (3)$$

where y_i is the equivalent concentration of gallic acid in ppm for the sample i ; x_i is the concentration of the extract sample i ; n is the number of samples; and c is the intercept value of the regression line between the equivalent concentration of gallic acid in ppm and the extract concentration in ppm. The value of milligrams of gallic acid equivalent per gram of extract is an estimate of the gradient of the regression line. All the experiments were conducted in triplicate.

2.7. Total Flavonoid Content

This assay was performed based on Chang et al., (2002) [41], with modification. A 0.5 mL sample was added to 1.5 mL of ethanol, 0.1 mL of 10% aluminum chloride, 0.1 mL of 1M sodium acetate, and 2.8 mL of distilled water. The mixed solution was vortexed and incubated at room temperature for 30 min and the absorbance was measured at maximum wavelength (434 nm) with the UV Spectrophotometer (Thermo Scientific Orion Aquamate 8000). The standard curve was made by replacing the sample with quercetin. The blank was created by replacing the sample with ethanol. All the experiments were conducted in triplicate.

The total flavonoid content result was expressed as milligrams of quercetin equivalent per gram of extract (similar to the units used in [39,42]). This value was obtained by using a similar formula to the total phenolic content, but now y_i is the concentration of quercetin equivalent (QE) in ppm, and c is the intercept value of the regression line between the quercetin acid equivalent in ppm and the extract concentration in ppm. Analogous to the total phenolic content, the value of milligrams of quercetin equivalent per gram of extract is an estimate of the gradient of the regression line.

2.8. Gas Chromatography—Mass Spectrometry (GC-MS) Analysis

The leaf and twig extracts of *A. sumatranus* were analyzed on the gas chromatography—mass spectrometer (Agilent 7890B GC and 5777A MSD), equipped with a capillary column (30 m \times 250 μm \times 0.25 μm , Agilent, type 19091S-433), set in the EI mode, at 70 eV. The temperature range of the oven was 40–300 °C. Helium was used as the carrier gas, and the volume of the injection was 1 μL . The identification of the compounds was made by

comparing the spectra to the NIST 2017 library. The derivatization of the sample was made using BSTFA (N,O-Bis(trimethylsilyl)trifluoroacetamide).

2.9. Liquid Chromatography—Mass Spectrometry (LC-MS-MS) Analysis

Each ethanol extract of the leaf and twig of *A. sumatranus* was analyzed using liquid chromatography mass spectrometer/mass spectrometer or LC-MS-MS (Waters Acquity UPLC I-Class and XEVO G2-XS QTof). One microliter of the sample was injected into the LC-MS-MS column using the gradient solvent (0.1% formic acid in water and 0.1% formic acid in acetonitrile). The column used C₁₈ 2.1 × 50 mm with a 1.7 μm particle size. The machine was set to scan from *m/z* 100 to *m/z* 1200 in the electron spray ionization (ESI) mode. The data obtained were processed by using the UNIFI software (Waters Corporation, Milford, MA, USA).

2.10. Docking Study

The α-glucosidase structure was taken from the PDB (<https://www.rcsb.org/>, accessed on 1 May 2022) using a 3A4A model. The missing atoms from the 3A4A model were recreated using Swiss Model (<https://swissmodel.expasy.org>, accessed on 1 May 2022). This 3A4A structure was used as the receptor. The ligand structures were obtained from the ZINC (<https://zinc.docking.org>, accessed on 1 May 2022) and PubChem (<https://pubchem.ncbi.nlm.nih.gov/>, accessed on 1 May 2022) databases. The receptor and ligand were prepared using AutoDock tools version 1.5.7, and the docking simulation was conducted using AutoDock version 4.2.6. [43], run on a computer with the following specifications: AMD Reizen 7 5800H, RAM 32 GB, and graphic card NVIDIA GeForce RTX 3060. In the simulation, the receptor was treated as a rigid object. The algorithm used in the simulation was the Lamarckian Genetic Algorithm (GA) with the following parameters: the number of GA runs was 100; the population size was 300; and the maximum number of evaluations was 2,500,000 for the ligands having a number of torsions fewer than 10, and 25,000,000 for those having a number of torsions greater than 10; this minimized the default scoring function of AutoDock 4.2.6. This default scoring function was an empirical approximation of the binding energy. The docking simulation was done on a rectangular grid of 126 × 126 × 126 with a grid size of 0.55 Å. The center of the rectangular grid was placed at the coordinate (21.301, −3.222, 18.662). In this way, the docking grid covered the whole receptor structure. These settings were verified by conducting a docking simulation with the native ligand of the 3A4A structure, which was GLC (obtained from PDB database). The docking result with the native ligand showed that the docking simulation could produce a docking result with RMSD 0.66 Å compared to the crystallography results.

3. Results and Discussion

3.1. Total Phenolic Content

The total phenolic content of the *A. sumatranus* leaf and twig ethanol extracts were 158.738 ± 8.615 mg GAE/g extract and 258.996 ± 17.462 mg GAE/g extract, respectively. It can also be confirmed in Figure 1 that the total phenolic content of the twig extract was higher than that of the leaf extract.

In the calculation of mg, the GAE/g must first be subtracted by the intercept value of the regression lines in Figure 1 to correct the bias (see Section 2.6). The bias appeared because the calibration regression line of the gallic acid concentration ($R^2 = 0.991$, see Figure S1) had a non-zero intercept.

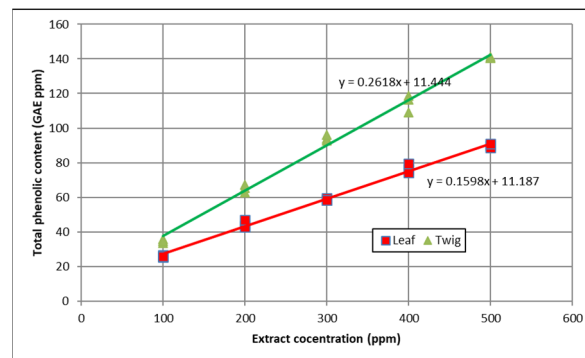


Figure 1. Total phenolic content of leaf and twig ethanol extract in GAE (gallic acid equivalent) ppm.

3.2. Total Flavonoid Content

The total flavonoid content of the *A. sumatranus* leaf and twig ethanol extracts were 38.521 ± 1.440 mg QE/g extract and 25.553 ± 2.394 mg QE/g extract, respectively. The graphs in Figure 2 confirm that the total flavonoid content of the twig extract was lower than that of the leaf extract. Considering the results of the total phenolic content in Section 3.1, it can be concluded that a large proportion of the phenolic compound in the twig extract was not flavonoid.

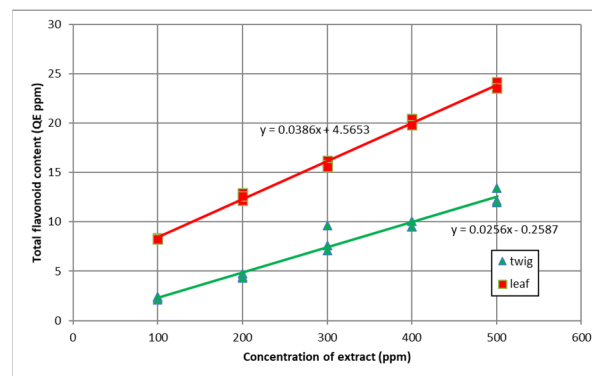


Figure 2. The total flavonoid content of leaf and twig ethanol extract in QE (quercetin equivalent) ppm.

As in the total phenolic content, the calculation of the total flavonoid content must also be corrected for bias by subtracting the intercept values of the regression lines in Figure 2 from the respective values of the quercetin acid equivalent concentration of the twig and leaf extracts (see Section 2.7). The reason is similarly based on the non-zero intercept value of the calibration regression line of the quercetin equivalent concentration ($R^2 = 0.998$, see Figure S2)

3.3. Ferric Reducing Antioxidant Power (FRAP)

The antioxidant activities of the leaf and twig ethanol extracts of *A. sumatranus* measured using the FRAP method were 0.0197 ± 0.0033 Fe²⁺ mol/g extract and 0.0173 ± 0.0009 Fe²⁺ mol/g extract, respectively. These values are quite small compared to the measured value for ascorbic acid, which was 0.1992 ± 0.0056 Fe²⁺ mol/g. The subtraction of the regression line intercept in the calculation of Fe²⁺ mol/g (see Section 2.5) was made to remove the bias, which appeared due to the non-zero intercept of the calibration regression line of the FRAP ($R^2 = 0.992$, see Figure S3). The comparison of the antioxidant activities in the ferric ion equivalent antioxidant activity (FeEAc) in mM can be seen in Figure 3, which verifies that the rate of increase in antioxidant activity of the leaf extract was a little bit higher than the twig extract, but both extracts had a lower rate of increase of antioxidant activities compared to ascorbic acid.

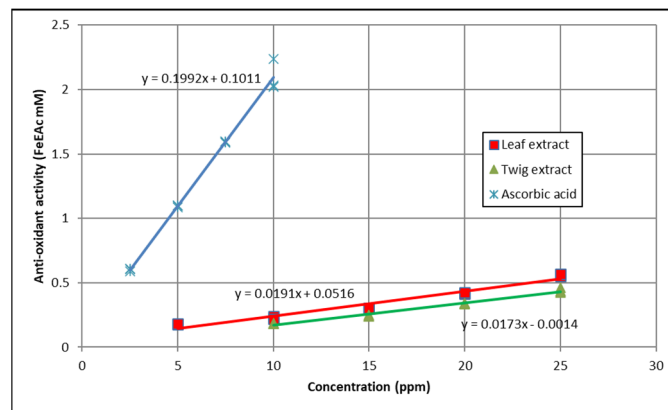


Figure 3. Ferric ion equivalent antioxidant activity (FeEAc) of leaf and twig ethanol extracts in ppm.

3.4. 2,2-Diphenyl-1-Picrylhydrazyl (DPPH) Radical Scavenging Activity

The antioxidant activities were also measured using a DPPH assay in this research. The results were presented as the IC₅₀ of the DPPH inhibition: 17.186 ppm for the leaf extract and 19.547 ppm for the twig extract. For comparison, the IC₅₀ of the ascorbic acid measured in this experiment was 10.604 ppm (60.17 μM). These values were obtained from the regression line of the percentage of DPPH inhibition with respect to the concentration in ppm, as shown in Figure 4. The respective R² values of the regression lines for the different entities were 0.993 (leaf extract), 0.993 (twig extract), and 0.980 (ascorbic acid).

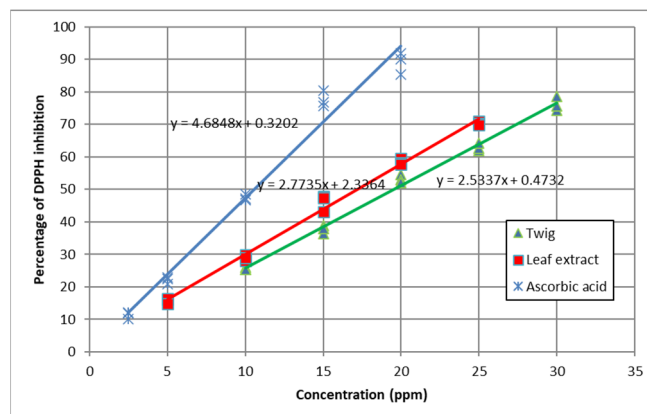


Figure 4. Percentage of free radical-scavenging capacities of leaf and twig ethanol extract in ppm measured in DPPH assay.

These DPPH results confirmed the conclusion of the FRAP assay results in Section 3.3. The antioxidant activity of the twig extract was lower than that of the leaf extract. Both extracts had lower antioxidant activities compared to the ascorbic acid. Nevertheless, considering the values of the IC₅₀, both extracts were quite strong antioxidant agents in comparison with the known strong antioxidant, ascorbic acid. The FRAP results also showed that the rate of increase in antioxidant activities for both extracts was lower than for ascorbic acid, making it harder to increase the inhibition of DPPH. This can also be seen in the lower gradient of the regression lines for the extracts in Figure 4, compared to the one for ascorbic acid.

3.5. α-Glucosidase Inhibition

The α-glucosidase inhibition activity of the leaf and twig ethanol extracts is shown in Figure 5. From the figure, it can be seen that the IC₅₀ value of the leaf (11.375 ppm) was smaller than the twig (16.378 ppm). This shows that the leaf ethanol extract was stronger

than that of the twig. Nevertheless, the IC₅₀ of both the leaf and twig ethanol extracts were weaker than the positive reference, quercetin (3.082 ppm or 10.19 μM).

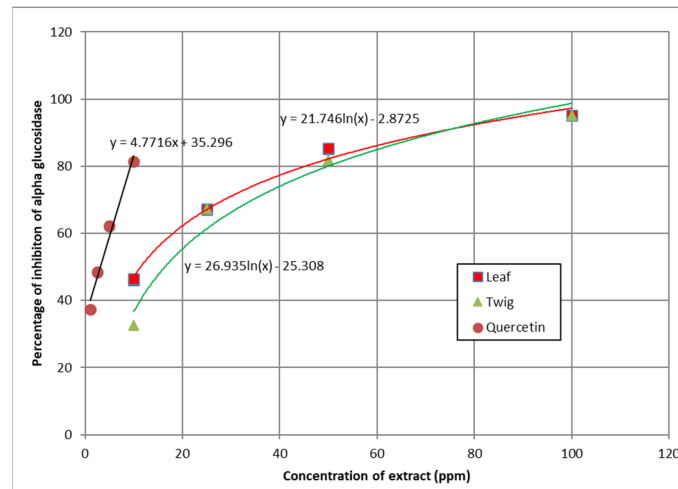


Figure 5. Percentage of α-glucosidase inhibition of leaf and twig ethanol extracts in ppm.

As can be seen in Figure 5, the data for the leaf and twig extracts are both approximated by logarithmic regression lines, which better fit the data than linear regression lines (R^2 for the logarithmic regression lines for the leaf and twig extracts are 0.990 and 0.969, respectively). The data for the positive reference, quercetin, was approximated with the linear regression line ($R^2 = 0.980$), which has a better fit than the logarithmic regression line for this case. These regression lines were used to compute the IC₅₀ values.

3.6. Gas Chromatography—Mass Spectrometry (GC-MS) Analysis

From the GC-MS, several compounds were identified from the twig ethanol extract, as can be seen in Figure 6 and Table 1. Based on the peak area, it can be deduced how much of the compound is available in the twig extract. However, this list of compounds is not yet exhaustive. These were just the compounds which could be identified using the database linked to the GC-MS machine and software. Similar lists for the identified compounds in the leaf ethanol extract using GC-MS can be seen in Figure 7 and Table 2.

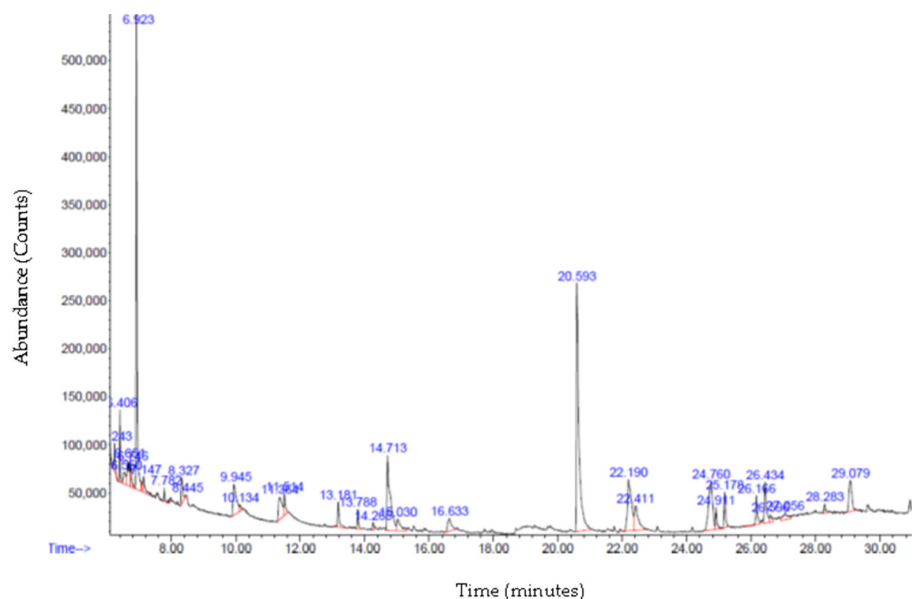
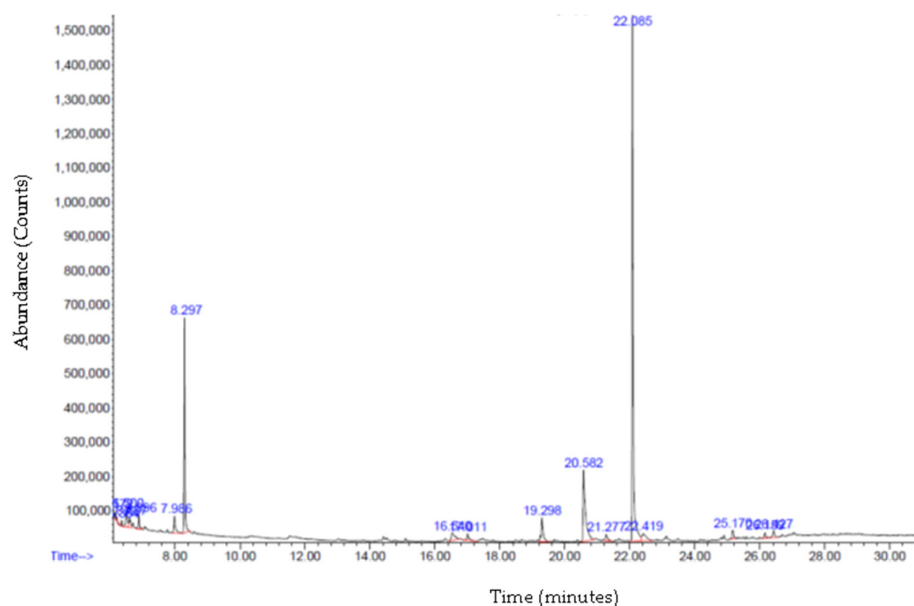


Figure 6. Gas Chromatography—Mass Spectrometry result of *Artabotrys sumatranus* twig extract.

Table 1. Identified compounds from GC-MS analysis of twig extract.

R/T	Compound	Formula	MW	Peak Area%
14.708	Naphthalene decahydro-4a-methyl-1-methylene-7-(1-methylethenyl)-, [4aR-trans]	C ₁₅ H ₂₄	204.4	8.8280
24.765	9-O-Pivaloyl-N-acetylcolchinol	C ₂₅ H ₃₁ NO ₆	441.5	6.9491
29.075	Anthracene, 9,10-dihydro-9,9,10-trimethyl	C ₁₇ H ₁₈	222.32	3.25
15.035	Zonarene	C ₁₅ H ₂₄	204.4	1.7401
13.183	Copaene	C ₁₅ H ₂₄	204.4	1.598
13.787	Caryophyllene	C ₁₅ H ₂₄	204.4	0.915
26.592	N-Methyl-1-adamantaneacetamide	C ₁₃ H ₂₁ NO	207.31	0.59
14.266	Lavandulyl isobutyrate	C ₁₅ H ₂₄	204.4	0.3354

Note: R/T = retention time, MW = molecular weight.

**Figure 7.** Gas Chromatography—Mass Spectrometry result of *Artabotrys sumatranus* leaf extract.**Table 2.** Identified compounds from GC-MS analysis of leaf extract.

R/T	Compound	Formula	MW	Peak Area%
19.295	7,9-Di-tert-butyl-1-oxaspiro(4,5)deca-6,9-diene-2,8-dione	C ₁₇ H ₂₄ O ₃	276.4	4.07
7.990	D- Limonene	C ₁₀ H ₁₆	136.2	2.29
21.274	Octacosane	C ₂₈ H ₅₈	394.8	1.09
17.014	Octadecane	C ₁₈ H ₃₈	254.5	1.03

Note: R/T = retention time, MW = molecular weight.

Most of the compounds found in the twig and leaf extracts using GC-MS were from the terpenoid group except anthracene, 9,10-dihydro-9,9,10-trimethyl, a phenolic compound (in the twig extract), and 7,9-Di-tert-butyl-1-oxaspiro(4,5)-deca-6,9-diene-2,8-dione, a flavonoid compound (in the leaf extract).

3.7. Liquid Chromatography—Mass Spectrometry (LC-MS/MS) Analysis

Compared to the GC-MS (see Tables 1 and 2), the identified compounds in the leaf and twig ethanol extracts of *A. sumatranus* from the LC-MS/MS results (see Table 3 and Figure 8, as well as Table 4 and Figure 9, respectively) had a higher molecular weight (MW). This was expected since the compounds identified in GC-MS were volatile, which usually have low molecular weights. This list was, of course, not exhaustive.

Table 3. Identified compounds from LC-MS/MS analysis for leaf extract.

R/T	Compound	Formula	Observed MW	Adduct	Response
2.68	Mangiferin	C ₁₉ H ₁₈ O ₁₁	423.09	+H, +Na	443421
3.23	Kaempferol 7-O- α -L-rhamnoside	C ₂₁ H ₂₀ O ₁₀	433.11	+H	157434
12.91	Stigmastan-3,6-dione	C ₂₉ H ₄₈ O ₂	429.4	+H	108634
2.24	Neomangiferin	C ₂₅ H ₂₈ O ₁₆	585.15	+H, +Na	100578
2.87	Asperuloside	C ₁₈ H ₂₂ O ₁₁	437.1	+Na	88206

Note: R/T = retention time, MW = molecular weight.

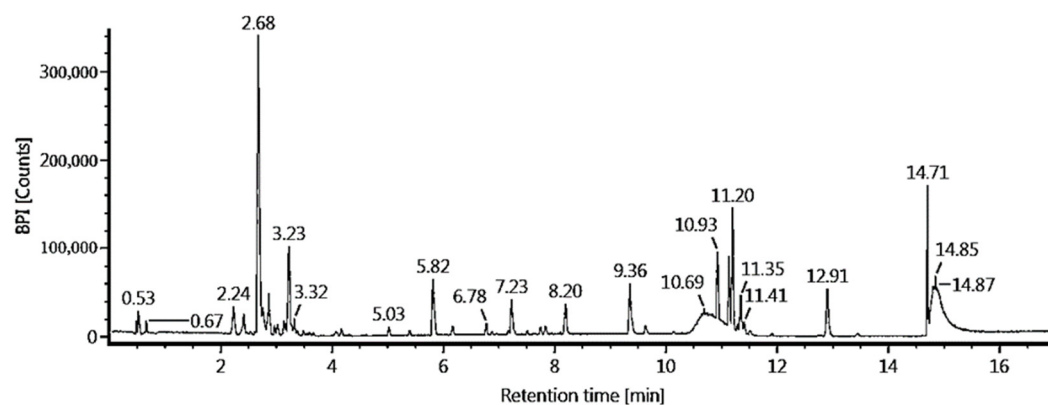


Figure 8. Liquid Chromatography—Mass Spectrometry/Mass Spectrometry result of *Artabotrys sumatranus* leaf extract (BPI = Base Peak Intensity).

Table 4. Identified compounds from LC-MS/MS analysis for twig extract.

R/T	Compound	Formula	Observed MW	Adduct	Response
2.67	Mangiferin	C ₁₉ H ₁₈ O ₁₁	423.09	+H, +Na	374611
9.36	Trichosanic acid	C ₂₉ H ₄₈ O ₂	279.23	+H	212382
2.21	Neomangiferin	C ₂₅ H ₂₈ O ₁₆	585.15	+H, +Na	193055
12.91	Stigmastan-3,6-dione	C ₂₉ H ₄₈ O ₂	429.4	+H	162276
4.07	Moupinamide	C ₂₁ H ₂₀ O ₁₀	433.11	+H	70497

Note: R/T = retention time, MW = molecular weight.

Some of the compounds identified in the LC-MS/MS were from the flavonoid groups, such as mangiferin and neomangiferin, in both the leaf and twig extracts. By observing the response, it could be deduced that mangiferin was the most abundant identified compound from the LC-MS-MS results for both the twig and leaf extracts, but it was more abundant in the leaf than in the twig extract. Neomangiferin was more abundant in the twig extract than in the leaf extract. For the leaf extract, there was another flavonoid compound identified, which was kaempferol 7-O- α -L-rhamnoside. The other identified compounds in the leaf and twig extracts, using the LC-MS-MS analysis, were mostly from the triterpenoid group.

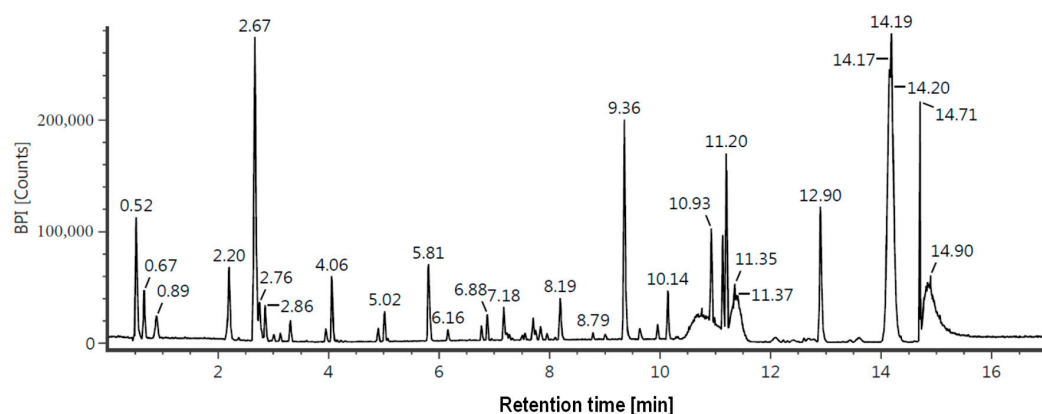


Figure 9. Liquid Chromatography—Mass Spectrometry/ Mass Spectrometry result of *Artabotrys sumatranus* twig extract (BPI = Base Peak Intensity).

3.8. Molecular Docking Results

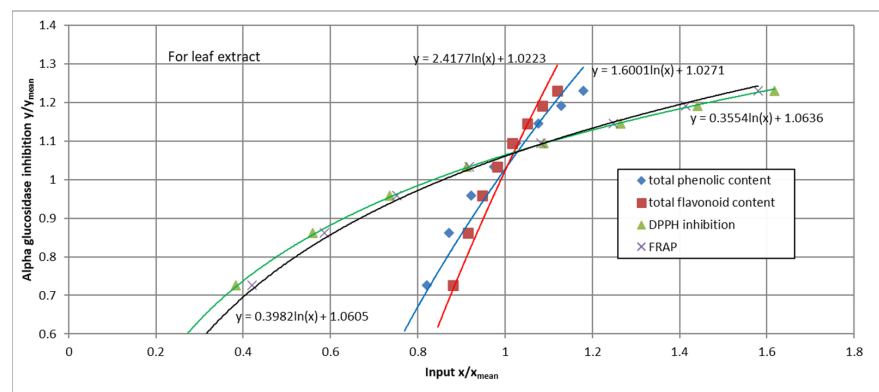
The molecular docking simulations for all the identified compounds from both the GC-MS and LC-MS-MS were conducted to find out whether these compounds have the potential to become α -glucosidase inhibitors. Here, the ligands were the identified compounds, while the receptor was the α -glucosidase enzyme. The results are shown in Table 5.

Table 5. Binding energy and inhibition constants values for ligand binding to α -glucosidase.

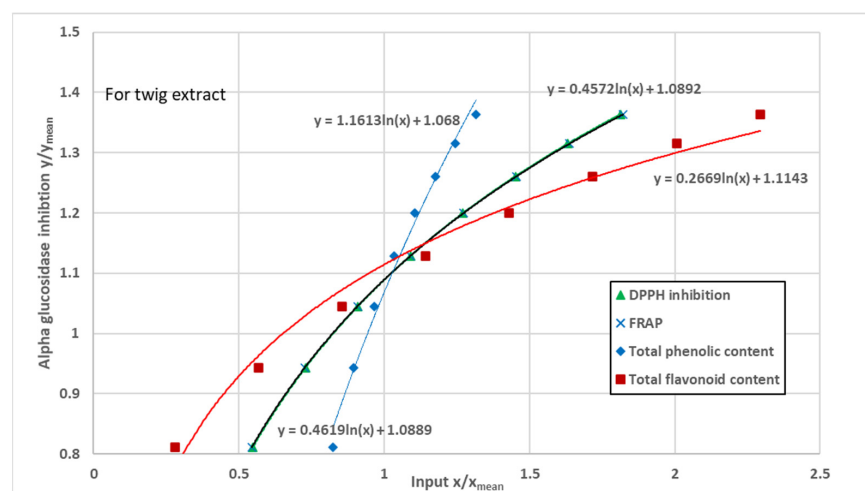
No.	Compound	Free Binding Energy (kcal/mol)	Inhibition Constant (K_i)
1	Neomangiferin	−16.27	1.18 pM
2	Kaempferol-7-O- α -L-rhamnoside	−12.86	372.97 pM
3	Asperuloside	−12.39	829.30 pM
4	Mangiferin	−12.23	1.08 nM
5	Moupinamide	−10.61	16.65 nM
6	9-O-Pivaloyl-N-acetylcolchinol	−10.02	45.40 nM
7	Stigmastan 3,6-dione	−9.65	84.60 nM
8	7,9-Di-tert-butyl-1-oxaspiro(4,5)deca-6,9-diene-2,8-dione	−8.98	262.18 nM
9	Trichosanic acid	−7.81	1.89 μ M
10	N-Methyl-1-adamantaneacetamide	−7.67	2.40 μ M
11	Anthracene, 9,10-dihydro-9,9,10-trimethyl	−7.62	2.59 μ M
12	Naphthalene decahydro-4a-methyl-1-methylene-7-(1-methylethenyl)-, [4aR-trans]	−7.51	3.10 μ M
13	Copaene	−7.34	4.18 μ M
14	Zonarene	−7.15	5.78 μ M
15	(β -)Caryophyllene	−7.00	6.12 μ M
16	Lavandulyl isobutyrate	−6.67	12.93 μ M
17	D limonene	−5.72	63.83 μ M
18	Octadecane	−5.53	88.13 μ M

4. Discussion

Since the samples taken for the different quantities could not have the same concentrations (due, for example, to the too-small measurement result values, e.g., the absorbance, making it unreliable), the comparison between the measured quantities (total phenolic content, total flavonoid content, antioxidant activity (DPPH and FRAP methods), and α -glucosidase inhibition) could not be conducted using a simple Pearson correlation. Therefore, to compare the different quantities, first, the regression lines, which were made between the measured quantities and the extract concentration (see Figures 1–5), were used to compute the measured quantities of the extract concentrations in the range of 5 ppm to 50 ppm, in increments of 5 ppm. Then, for the extract concentrations, the regression lines between the α -glucosidase inhibition, as the output (y axis), and the rest of the measured quantities, as inputs (x axis), were made to identify which measured quantities had the strongest relationship to α -glucosidase inhibition (see Figure 10). To remove the scaling factor, the quantities were divided by their respective mean values. Similar plots were also made with DPPH inhibition (Figure 11) to find out which measured quantities had the strongest influence on the DPPH inhibition. For α -glucosidase inhibition, the regression lines were made with a logarithmic scale, since the α -glucosidase inhibition data are rather curved (see Figure 5). For the DPPH, the linear regression lines were a good fit to the data (see Figure 11), except when α -glucosidase inhibition is the input, due the same reason as above.

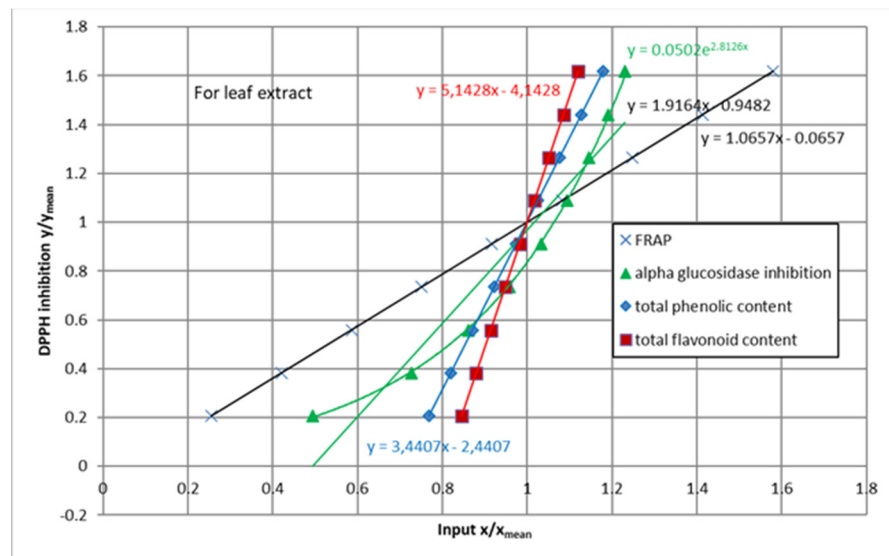


(a)

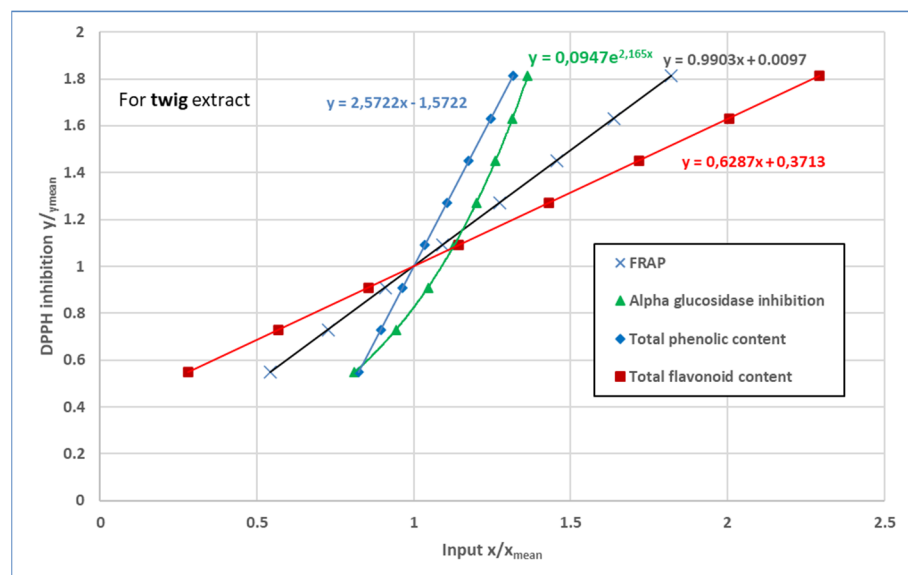


(b)

Figure 10. Comparison between α -glucosidase inhibition and several measured quantities: total phenolic content, total flavonoid content, DPPH (2,2-diphenyl-1-picrylhydrazyl) inhibition, and FRAP (ferric reducing antioxidant power) stated in ferric ion equivalent antioxidant activity, for leaf extract (a) and twig extract (b).



(a)



(b)

Figure 11. Comparison between DPPH (2,2-diphenyl-1-picrylhydrazyl) radical scavenging activity and several measured quantities: FRAP (ferric reducing antioxidant power), stated in in ferric ion equivalent antioxidant activity, α -glucosidase inhibition, total phenolic content, and total flavonoid content, for leaf extract (a) and twig extract (b).

From Figure 10a, for the leaf extract, the factors that had the strongest relationship to α -glucosidase inhibition (had the largest gradients) were the total flavonoid content and total phenolic content. The antioxidant activity had a weaker relationship to the α -glucosidase inhibition, both for the FRAP and DPPH results. Interestingly, for the twig extract (Figure 10b), only the total phenolic content had a strong relationship to the α -glucosidase inhibition. The FRAP and DPPH results for the twig extract showed a similar relationship to the α -glucosidase inhibition as for the leaf extract, stronger than that of the total flavonoid content. From these results, it could be deduced that the phenolic and flavonoid compounds in the leaf extracts were likely to have α -glucosidase inhibition activity. For the twig extract, the phenolic compounds were likely to be active, while the

flavonoids were probably not. It also seemed that the antioxidant agent did not necessarily have a strong α -glucosidase inhibition in both the leaf and twig extracts.

On the other hand, by observing Figure 11a, it could be deduced that, for the leaf extract, the total phenolic content, total flavonoid content, and α -glucosidase inhibition had a strong relationship to the DPPH results. The FRAP results had a gradient near 1, implying that the FRAP and DPPH were similar (one-to-one), which was expected since the FRAP and DPPH methods measured the same quantity. For the twig extract (see Figure 11b), the strong factors in the DPPH result were only the total phenolic content and α -glucosidase inhibition, while the total flavonoid content had a weaker relationship. The FRAP and DPPH results showed the same, nearly one-to-one, relationship as for the leaf extract. These results imply that the phenolic and flavonoid compounds in the leaf extract were likely active as antioxidant agents. It also seems that the active compounds for α -glucosidase inhibition in the leaf extract were also active as antioxidants. This result was not the same for the twig extract, where the active antioxidants are likely phenolic compounds, not flavonoid compounds. However, the inhibitor of α -glucosidase in the twig extract has a good chance to also have antioxidant activity, as with the leaf extract.

The activity potential as an α -glucosidase inhibitor increases as the binding energy becomes more negative, and the inhibition constant decreases. High-affinity binding can be defined as having an inhibition constant $K_i, \leq 250$ nM or binding energy ≤ -9 kcal/mol [44]. As can be seen in Table 5, the seven highest potential compounds that can be classified as having a high affinity to α -glucosidase are neomangiferin, kaempferol-7-O- α -L-rhamnoside, asperuloside, mangiferin, moupinamide, 9-O-Pivaloyl-N-acetylcolchinol, and stigmastan 3,6-dione. Some of these compounds have been verified by previous researchers as α -glucosidase inhibitors: neomangiferin and mangiferin [45], kaempferol-7-O- α -L-rhamnoside [46], asperuloside [47], and moupinamide [48]. The activity of 9-O-Pivaloyl-N-acetylcolchinol and stigmastan 3,6-dione to inhibit α -glucosidase has not yet been verified. Stigmastan was identified elsewhere as one of the compounds in an extract that showed good α -glucosidase inhibition [49], but has not yet been tested as a single compound.

Interestingly, some of the verified α -glucosidase inhibitor compounds (neomangiferin and mangiferin [45], kaempferol-7-O- α -L-rhamnoside [49], asperuloside [50], and moupinamide [51]) have also been shown to exhibit antioxidant activities. Whereas 9-O-Pivaloyl-N-acetylcolchinol and stigmastan 3,6-dione have not yet been verified before as antioxidant agents, stigmastan has been mentioned elsewhere as one of the compounds in an extract with good antioxidant activity [52]. This seems to corroborate the deduction made above: the α -glucosidase inhibitors in the leaf and twig ethanol extracts were likely also antioxidant agents. This relationship seems to be observed in other plants, such as in the research by Sekhon-Loodu and Rupasinghe (2019) [10], which found the correlation between α -glucosidase inhibition and antioxidant activity in *Myrica gale* and *Rhodiola rosea* extracts; and in similar findings by Pieczykolan, et al., (2021) [53], who conducted the research on *Aerva lanata* (L.) Juss.

The other deductions could not yet be convincingly verified, since the list of identified compounds is not yet exhaustive. Nevertheless, from the list in Table 5, some of the compounds are flavonoids: neomangiferin, kaempferol-7-O- α -L-rhamnoside, mangiferin, and 7,9-Di-tert-butyl-1-oxaspiro(4,5)deca-6,9-diene-2,8-dione. These are compounds with high and medium activities, shown in Table 5. By comparing these compounds with Tables 1–4, it can be seen that more of these flavonoids were found in the leaf extract than in the twig. This seems to support the deduction above that more flavonoids in the leaf extract were inhibitors of α -glucosidase than in the twig. Since all flavonoids are also phenolic compounds, the above deduction—that the phenolic compounds in the leaf extract were likely to be active—seems to be corroborated. Nevertheless, the deduction that, in the twig extract, only the phenolics compounds tend to be active while the flavonoids are not, seems not to be supported, since there were flavonoids which were active in the twig extract, although there was one phenolic compound found in the twig extract but not in the leaf extract, anthracene (but its activity as an α -glucosidase inhibitor was not very strong).

Perhaps the deduction could still be supported if more compounds in the twig extract were identified.

5. Conclusions

In Vitro and in silico analyses of *A. sumatranus* leaf and twig ethanol extracts showed their potential as α -glucosidase inhibitors, although the activity was caused by different group of compounds. It seems that both phenolic and flavonoid compounds contribute to the activity of α -glucosidase inhibition in both the leaf and twig ethanol extracts. The comparisons between the antioxidant and α -glucosidase inhibition activities also indicated that the compounds with a high affinity to α -glucosidase were likely to have antioxidant activity, too. The molecular docking analysis on the LC MS/MS data showed that the major compound in both extracts with the highest affinity to α -glucosidase was neomangiferin.

Supplementary Materials: The following supporting information can be downloaded at: <https://www.mdpi.com/article/10.3390/scipharm91010002/scipharm91010002/s1>, Figure S1: Calibration curve of gallic acid equivalent (GAE) for total phenolic content; Figure S2: Calibration curve of quercetin equivalent (QE) for total flavonoid content; Figure S3: Calibration curve of iron (II) sulphate.

Author Contributions: D.R. performed the experiment and wrote the manuscript; B.E. designed the experiment and reviewed the article; M.H. and M.I.S. collected the samples, conducted the LC-MS/MS and GC-MS analyses, and reviewed the article; A.K. reviewed the article. All authors have read and agreed to the published version of the manuscript.

Funding: This research was funded by Pelita Harapan University through internal grant number P-03-FIKes/XII/2021.

Institutional Review Board Statement: Not applicable.

Informed Consent Statement: Not applicable.

Data Availability Statement: Not applicable.

Acknowledgments: We thank the Cibodas Botanical Garden for providing the samples, the National Research and Innovation Institutes for the study funding through the Degree by Research Scholarship, the Advanced Characterization Laboratories Serpong at the National Research and Innovation Institute, and the Pharmaceutical Biology Laboratory at Pelita Harapan University for the research facilities, as well as scientific and technical support.

Conflicts of Interest: The authors declare no conflict of interest.

References

1. Wei, J.; Tian, J.; Tang, C.; Fang, X.; Miao, R.; Wu, H.; Wang, X.; Tong, X. The influence of different types of diabetes on vascular complications. *J. Diabetes Res.* **2022**, *2022*, 3448618. [[CrossRef](#)] [[PubMed](#)]
2. Padhi, S.; Kumar, A.; Behera, A. Biomedicine & pharmacotherapy type II diabetes mellitus: A review on recent drug based therapeutics. *Biomed. Pharmacother.* **2020**, *131*, 110708. [[CrossRef](#)] [[PubMed](#)]
3. Dirir, A.M.; Daou, M.; Yousef, A.F.; Yousef, L.F. A review of alpha-glucosidase inhibitors from plants as potential candidates for the treatment of type-2 diabetes. *Phytochem. Rev.* **2021**, *21*, 1049–1079. [[CrossRef](#)] [[PubMed](#)]
4. Mehta, A.; Zitzmann, N.; Rudd, M.P.; Bock, M.T.; Dwek, A.R. Alpha glucosidase inhibitors as potential broad based anti-viral agents. *FEBS Lett.* **1998**, *430*, 17–22. [[CrossRef](#)]
5. Zhao, Y.; Wang, Y.; Lou, H.; Shan, L. Alpha-glucosidase inhibitors and risk of cancer in patients with diabetes mellitus: A systematic review and meta-analysis. *Oncotarget* **2017**, *8*, 81027–81039. [[CrossRef](#)] [[PubMed](#)]
6. Khwaja, N.U.D.; Arunagirinathan, G. Efficacy and cardiovascular safety of alpha glucosidase inhibitors. *Curr. Drug Saf.* **2021**, *16*, 122–128. [[CrossRef](#)] [[PubMed](#)]
7. Krentz, A.J. Evolution of glucose-lowering drugs for type 2 diabetes: A new era of cardioprotection. In *Nutritional and Therapeutic Interventions for Diabetes and Metabolic Syndrome*; Elsevier Inc.: Amsterdam, The Netherlands, 2018; pp. 429–454. ISBN 9780128120194.
8. Rosa, M.M.; Dias, T. Commonly used endocrine drugs. *Handb. Clin. Neurol.* **2014**, *120*, 809–824. [[CrossRef](#)]
9. Hossain, M.A.; Pervin, R. Current antidiabetic drugs. In *Nutritional and Therapeutic Interventions for Diabetes and Metabolic Syndrome*; Elsevier Inc.: Amsterdam, The Netherlands, 2018; pp. 455–473. ISBN 9780128120194.
10. Sekhon-Loodu, S.; Rupasinghe, H.P.V. Evaluation of antioxidant, antidiabetic and antiobesity potential of selected traditional medicinal plants. *Front. Nutr.* **2019**, *6*, 53. [[CrossRef](#)]

11. Ibrahim, M.A.; Koorbanally, N.A.; Islam, M.S. Antioxidative activity and inhibition of key enzymes linked to type-2 diabetes (α -glucosidase and α -amylase) by *Khaya senegalensis*. *Acta Pharm.* **2014**, *64*, 311–324. [[CrossRef](#)]
12. Galicia-Garcia, U.; Benito-Vicente, A.; Jebari, S.; Larrea-Sebal, A.; Siddiqi, H.; Uribe, K.B.; Ostolaza, H.; Martín, C. Pathophysiology of type 2 diabetes mellitus. *Int. J. Mol. Sci.* **2020**, *21*, 6275. [[CrossRef](#)]
13. Kumar, S.; Narwal, S.; Kumar, V.; Prakash, O. α -glucosidase inhibitors from plants: A natural approach to treat diabetes. *Pharmacogn. Rev.* **2011**, *5*, 19–29. [[CrossRef](#)] [[PubMed](#)]
14. Anwar, H.; Hussain, G.; Mustafa, I. Antioxidants from natural sources. In *Antioxidants in Foods and Its Application*; IntechOpen: London, UK, 2018; pp. 3–28. [[CrossRef](#)]
15. Rasheed, A.; Fathima Abdul Azeez, R. A review on natural antioxidants. In *Traditional and Complementary Medicine*; IntechOpen: London, UK, 2019. [[CrossRef](#)]
16. Cedeño, H.; Espinosa, S.; Andrade, J.M.; Cartuche, L.; Malagon, O. Novel flavonoid glycosides of quercetin from leaves and flowers of *Gaiadendron punctatum* G.Don (Violeta de Campo), used by the saraguro community in Southern Ecuador, inhibit alpha glucosidase enzyme. *Molecules* **2019**, *24*, 4267. [[CrossRef](#)] [[PubMed](#)]
17. Mosihuzzman, M.; Naheed, S.; Hareem, S.; Talib, S.; Abbas, G.; Khan, S.N.; Choudhary, M.I.; Sener, B.; Tareen, R.B.; Israr, M. Studies on α -glucosidase inhibition and anti-glycation potential of *Iris loczyi* and *Iris unguicularis*. *Life Sci.* **2013**, *92*, 187–192. [[CrossRef](#)]
18. Alqahtani, A.S.; Hidayathulla, S.; Rehman, M.T.; Elgamal, A.A.; Al-Massarani, S.; Razmovski-Naumovski, V.; Alqahtani, M.S.; El Dib, R.A.; Alajmi, M.F. Alpha-amylase and alpha-glucosidase enzyme inhibition and antioxidant potential of 3-oxolupenal and katononic acid isolated from *Nuxia oppositifolia*. *Biomolecules* **2020**, *10*, 61. [[CrossRef](#)] [[PubMed](#)]
19. Gao, H.; Huang, Y.N.; Gao, B.; Li, P.; Inagaki, C.; Kawabata, J. Inhibitory effect on α -glucosidase by *Adhatoda vasica* Nees. *Food Chem.* **2008**, *108*, 965–972. [[CrossRef](#)]
20. Sheikh, Y.; Chanu, M.B.; Mondal, G.; Manna, P.; Chattoraj, A.; Chandra Deka, D.; Chandra Talukdar, N.; Chandra Borah, J. Procyanidin A2, an anti-diabetic condensed tannin extracted from *Wendlandia glabrata*, reduces elevated G-6-Pase and mRNA levels in diabetic mice and increases glucose uptake in CC1 hepatocytes and C1C12 myoblast cells. *RSC Adv.* **2019**, *9*, 17211–17219. [[CrossRef](#)]
21. Yoshikawa, M.; Murakami, T.; Yashiro, K.; Matsuda, H. Kotalanol, a potent alpha glukosidase inhibitor with thiosugar sulfonium sulfate structure, from antidiabetic Ayurvedic medicine *Salacia reticulata*. *Chem. Pharm. Bull.* **1998**, *46*, 1339–1340. [[CrossRef](#)]
22. Yoshikawa, M.; Nishida, N.; Shimoda, H.; Takada, M.; Kawahara, Y.; Matsuda, H. Polyphenol constituents from *Salacia* Species: Quantitative analysis of mangiferin with α -glucosidase and aldose reductase inhibitory activities. *Yakugaku Zasshi* **2001**, *121*, 371–378. [[CrossRef](#)]
23. Hung, N.H.; Dai, D.N.; Dung, D.M.; Giang, T.T.B.; Thang, T.D.; Ogunwande, I.A. Chemical composition of essential oils of *Artabotrys petelotii* Merr., *Artabotrys intermedius* Hassk., and *Artabotrys harmandii* Finet & Gagnep. (Annonaceae) from Vietnam. *J. Essent. Oil-Bear. Plants* **2014**, *17*, 1105–1111. [[CrossRef](#)]
24. Chen, J.; Eiadthong, W. New species and new records of *Artabotrys* (Annonaceae) from peninsular Thailand. *PhytoKeys* **2020**, *151*, 67–81. [[CrossRef](#)]
25. Chong, J.Y.; Rajagopal, M.; Chandramanthi, S.; Ashok Kumar, B.; Sasikala, C.; Geethanjali, K. Evaluation of antibacterial activity against multidrug resistant (MDR) bacteria by the fractions of *Artabotrys suaveolens* (Blume). *Curr. Trends Biotechnol. Pharm.* **2020**, *15*, 262–269. [[CrossRef](#)]
26. Mohan, S.K.; Veeraraghavan, V.P.; Balakrishna, J.P.; Rengasamy, G.; Rajeshkumar, S. Antidiabetic activity of methanolic extract of *Artabotrys suaveolens* Leaves in 3T3-L1 cell line. *J. Pure Appl. Microbiol.* **2020**, *14*, 573–580. [[CrossRef](#)]
27. Kwan, T.K.; Shipton, F.; Nor Azman, N.S.; Hossan, S.; Jin, K.T.; Wiart, C. Cytotoxic aporphines from *Artabotrys crassifolius*. *Nat. Prod. Commun.* **2016**, *11*, 389–392. [[CrossRef](#)]
28. Liu, Y.P.; Tang, J.Y.; Hua, Y.; Lai, L.; Luo, X.L.; Zhang, Z.J.; Yin, W.Q.; Chen, G.Y.; Fu, Y.H. Bioactive polyoxygenated seco-cyclohexenes from *Artabotrys hongkongensis*. *Bioorg. Chem.* **2018**, *76*, 386–391. [[CrossRef](#)]
29. Wen, Q.; Liu, Y.P.; Yan, G.; Yang, S.; Hu, S.; Hua, J.; Yin, W.Q.; Chen, G.Y.; Fu, Y.H. Bioactive eudesmane sesquiterpenes from *Artabotrys hongkongensis* Hance. *Nat. Prod. Res.* **2020**, *34*, 1687–1693. [[CrossRef](#)]
30. Nyandoro, S.S.; Joseph, C.C.; Nkunya, M.H.H.; Hosea, K.M.M. New antimicrobial, mosquito larvicidal and other metabolites from two *Artabotrys* species. *Nat. Prod. Res.* **2013**, *27*, 1450–1458. [[CrossRef](#)]
31. Tan, K.K.; Khoo, T.J.; Rajagopal, M.; Wiart, C. Antibacterial alkaloids from *Artabotrys crassifolius* Hook.f. & Thomson. *Nat. Prod. Res.* **2015**, *29*, 2346–2349. [[CrossRef](#)]
32. Dewi, R.T.; Tachibana, S.; Darmawan, A. Effect on α -glucosidase inhibition and antioxidant activities of butyrolactone derivatives from *Aspergillus terreus* MC751. *Med. Chem. Res.* **2014**, *23*, 454–460. [[CrossRef](#)]
33. González-Palma, I.; Escalona-Buendía, H.B.; Ponce-Alquicira, E.; Téllez-Téllez, M.; Gupta, V.K.; Díaz-Godínez, G.; Soriano-Santos, J. Evaluation of the antioxidant activity of aqueous and methanol extracts of *Pleurotus ostreatus* in different growth stages. *Front. Microbiol.* **2016**, *7*, 1099. [[CrossRef](#)]
34. Tomasina, F.; Carabio, C.; Celano, L. Analysis of two methods to evaluate antioxidants. *Biochem. Mol. Biol. Educ.* **2012**, *40*, 266–270. [[CrossRef](#)]
35. Wiliantari, S.; Iswandana, R.; Elya, B. Total polyphenols, total flavonoids, antioxidant activity and inhibition of tyrosinase enzymes from extract and fraction of *Passiflora ligularis* Juss. *Pharmacogn. J.* **2022**, *14*, 660–671. [[CrossRef](#)]

36. Irshad, M.; Zafaryab, M.; Singh, M.; Rizvi, M.M.A. Comparative analysis of the antioxidant activity of cassia fistula extracts. *Int. J. Med. Chem.* **2012**, *2012*, 157125. [[CrossRef](#)]
37. Budiarmo, F.S.; Elya, B.; Hanafi, M.; Limengan, A.H.; Rahmasari, R. Antioxidant activity of methanol fractions stem bark of Kayu Sarampa (*Xylocarpus moluccensis* (Lam.) M. Roen)). *Pharmacogn. J.* **2021**, *13*, 1694–1701. [[CrossRef](#)]
38. Chavan, J.J.; Gaikwad, N.B.; Kshirsagar, P.R.; Dixit, G.B. Total phenolics, flavonoids and antioxidant properties of three *Ceropegia* species from Western Ghats of India. *South African J. Bot.* **2013**, *88*, 273–277. [[CrossRef](#)]
39. Rahim, N.A.; Roslan, M.N.F.; Muhamad, M.; Seeni, A. Antioxidant activity, total phenolic and flavonoid content and LC–MS profiling of leaves extracts of *Alstonia angustiloba*. *Separations* **2022**, *9*, 234. [[CrossRef](#)]
40. Molole, G.J.; Gure, A.; Abdissa, N. Determination of total phenolic content and antioxidant activity of *Commiphora mollis* (Oliv.) Engl. Resin. *BMC Chem.* **2022**, *16*, 48. [[CrossRef](#)]
41. Chang, C.C.; Yang, M.H.; Wen, H.M.; Chern, J.C. Estimation of total flavonoid content in propolis by two complementary colorimetric methods. *J. Food Drug Anal.* **2002**, *10*, 178–182. [[CrossRef](#)]
42. Aryal, S.; Baniya, M.K.; Danekhu, K.; Kunwar, P.; Gurung, R.; Koirala, N. Total phenolic content, flavonoid content and antioxidant potential of wild vegetables from Western Nepal. *Plants* **2019**, *8*, 96. [[CrossRef](#)]
43. Morris, G.M.; Ruth, H.; Lindstrom, W.; Sanner, M.F.; Belew, R.K.; Goodsell, D.S.; Olson, A.J. Software news and updates AutoDock4 and AutoDockTools4: Automated docking with selective receptor flexibility. *J. Comput. Chem.* **2009**, *30*, 2785–2791. [[CrossRef](#)]
44. Morris, A.S.C.; Denham, A.S.; Bassett, H.H.; Curby, W.T. Differences between high- and low-affinity complexes of enzymes and non-enzymes. *J. Med. Chem.* **2008**, *51*, 6432–6441. [[CrossRef](#)]
45. Wang, J.; Lou, Z.; Zhu, Z.; Chai, Y.; Wu, Y. A Rapid high-performance liquid chromatographic method for quantitative analysis of antidiabetic-active components in *Anemarrhena asphodeloides* rhizomes. *Chromatographia* **2005**, *61*, 633–636. [[CrossRef](#)]
46. Chen, H.; Ouyang, K.; Jiang, Y.; Yang, Z.; Hu, W.; Xiong, L.; Wang, N.; Liu, X.; Wang, W. Analysis of the ethanol extracts of *Chimonanthus nitens* Oliv. leaves and their inhibitory effect on alpha -glucosidase activity. *Int. J. Biol. Macromol.* **2017**, *98*, 829–836. [[CrossRef](#)]
47. Koia, J.H.; Shepherd, P. The potential of anti-diabetic rākau rongoā (Māori herbal medicine) to treat type 2 diabetes mellitus (T2DM) mate huka: A review. *Front. Pharmacol.* **2020**, *11*, 935. [[CrossRef](#)]
48. Fan, P.; Terrier, L.; Hay, A.; Marston, A.; Hostettmann, K. Fitoterapia antioxidant and enzyme inhibition activities and chemical profiles of *Polygonum sachalinensis* F.Schmidt ex Maxim (Polygonaceae). *Fitoterapia* **2010**, *81*, 124–131. [[CrossRef](#)]
49. Xie, J.H.; Dong, C.J.; Nie, S.P.; Li, F.; Wang, Z.J.; Shen, M.Y.; Xie, M.Y. Extraction, chemical composition and antioxidant activity of flavonoids from *Cyclocarya paliurus* (Batal.) Iljinskaja leaves. *Food Chem.* **2015**, *186*, 97–105. [[CrossRef](#)]
50. Manzione, M.G.; Martorell, M.; Sharopov, F.; Ganesh, N.; Venkatesh, N.; Kumar, A.; Valere, P.; Fokou, T.; Pezzani, R. Phytochemical and pharmacological properties of asperuloside, a systematic review. *Eur. J. Pharmacol.* **2020**, *883*, 173344. [[CrossRef](#)]
51. Wang, Y.H. Traditional uses and pharmacologically active constituents of dendrobium plants for dermatological disorders: A review. *Nat. Products Bioprospect.* **2021**, *11*, 465–487. [[CrossRef](#)]
52. Khan, K.; Firdous, S.; Ahmad, A.; Fayyaz, N.; Rasheed, M.; Faizi, S. GC-MS profile of antimicrobial and antioxidant fractions from *Cordia rothii* roots. *Pharm. Biol.* **2016**, *54*, 2597–2605. [[CrossRef](#)]
53. Pieczykolan, A.; Pietrzak, W.; Gawlik-Dziki, U.; Nowak, R. Antioxidant, anti-inflammatory, and anti-diabetic activity of phenolic acids fractions obtained from *Aerva lanata* (L.) Juss. *Molecules* **2021**, *26*, 3486. [[CrossRef](#)]

Disclaimer/Publisher’s Note: The statements, opinions and data contained in all publications are solely those of the individual author(s) and contributor(s) and not of MDPI and/or the editor(s). MDPI and/or the editor(s) disclaim responsibility for any injury to people or property resulting from any ideas, methods, instructions or products referred to in the content.